Surface Water Mixing in the Solomon Sea as Documented by a High-Resolution Coral ^{14}C Record

T. P. GUILDERSON*

Center for Accelerator Mass Spectrometry, Lawrence Livermore National Laboratory, Livermore, California

D. P. SCHRAG

Laboratory for Geochemical Oceanography and the Department of Earth and Planetary Sciences, Harvard University, Cambridge, Massachusetts

M. A. CANE

Lamont-Doherty Earth Observatory and the Department of Earth and Environmental Sciences, Columbia University, Palisades, New York

(Manuscript received 19 March 2001, in final form 17 July 2003)

ABSTRACT

A bimonthly coral-based record of the postbomb radiocarbon content of Solomon Sea surface waters is interpreted to reflect mixing of subtropical surface water and that advected in from the east by the equatorial branch of the South Equatorial Current (SEC). Annual mean $\Delta^{14}C$ has a dynamic range of nearly 175‰, with a total range of nearly 200‰. Prebomb values average −56‰ and the annual mean postbomb maxima occurs in 1985 with a value of +117%. Interannual variability in the record reflects surface current variations in conjunction with surface wind changes associated with ENSO. During El Niño years the waters of the Solomon Sea reflect a stronger influence of waters advected in from the east by the SEC and less ''pure'' subtropical water. This is most likely accomplished by a southward shift of the equatorward branch of the SEC during El Niño. There is an overall decrease in the relative proportion of eastern tropical water that is interpreted as a decrease in the strength and intensity of the shallow circulation of the tropical Pacific during the latter portion of the twentieth century. If validated, this secular trend bears strongly upon the rate of extratropical–tropical recirculation and the redistribution of heat and salt within the tropical Pacific.

1. Introduction

The western tropical Pacific plays an important role in the localization of deep atmospheric convective activity and is a major exporter of latent and sensible heat to both hemispheres (e.g., Peixoto and Oort 1992). On interannual (e.g., El Niño–Southern Oscillation) and longer time scales the transport of warm surface water into and out of the western equatorial Pacific is thought to play an important role not only in regulating the development and termination of warm ENSO events, but also in global climate through atmospheric teleconnections. Compensation of westward flowing currents occurs via the surface countercurrents, eastward flowing undercurrents, and the Indonesian Throughflow (e.g., Goriou and Toole 1993). Our understanding of the interaction between the overlying wind field (the observations of which have their own problems; e.g., Luther and Harrison 1984; Clarke and Lebedev 1996) and the shallow circulation has historically relied upon data from ship drifts, drogues, and a relatively small number of current meter moorings (e.g., Reverdin et al. 1994). The paucity of data requires broad scale or coarse synoptic averaging and does not allow for more detailed questions regarding interannual to decadal-scale variability. Satellite observations such as scatterometer winds and altimeter data provide higher spatial and temporal sampling (e.g., Lagerloef et al. 1999) but are relegated to only the last 10–20 years. Such a time history is insufficient to look at longer time scale variability or to address such questions as anthropogenic influences on climate variability.

Subannual radiocarbon measurements of coral skeletal material that accurately record the $\Delta^{14}C$ of ΣCO_2 (e.g., Druffel 1981; Toggweiler et al. 1991; Guilderson

* Additional affiliation: Department of Ocean Sciences and Institute of Marine Sciences, University of California, Santa Cruz, Santa Cruz, California.

Corresponding author address: Dr. Thomas P. Guilderson, Center for Accelerator Mass Spectrometry, Lawrence Livermore National Laboratory, Livermore, CA 94551.
E-mail: guilderson1@llnl.gov

et al. 1998) have added important information to water sampling programs like Geochemical Ocean Sections (GEOSECS; Östlund et al. 1987) and the World Ocean Circulation Experiment (WOCE; Key et al. 1996). Although the WOCE program continues to produce seawater ^{14}C analysis today, there are notable limitations to shipboard sampling, primarily the inability to continuously monitor ocean conditions. For ^{14}C in the deep ocean, this is not a problem because the transport is relatively slow and the gradients are relatively low. For the surface ocean, where ^{14}C gradients are highest and transport is rapid, it has been demonstrated that temporal variability is of the same order as spatial variability (e.g., Guilderson et al. 1998), an observation which is lost in discrete analyses like GEOSECS or WOCE whose ''snapshots'' of bomb-radiocarbon are integrations of ~20 and ~40 years (respectively) of ocean dynamics. Atmospheric nuclear weapons testing in the late 1950s and early 1960s resulted in an excess of ^{14}C in the atmosphere and, as this signature has penetrated the ocean, it has augmented the natural gradient between the surface and deeper waters. Over the time frame of interest radioactive decay is negligible. Isotopic equilibration with the atmosphere is on the order of a decade (Broecker and Peng 1982). Thus, $\Delta^{14}C$ is a quasi-conservative, passive advective tracer, and time series such as those derived from archives, such as hermatypic corals, can augment historical, conventional (temperature, salinity) observations especially in times and regions where observations are sparse. Corals act like strip-recorders continuously recording the radiocarbon content of the waters in which they live and thus it is possible to use records derived from these biogenic archives to study ocean mixing (Guilderson et al. 1998; Druffel and Griffin 1999) and vertical exchange processes (Guilderson and Schrag 1998; Guilderson et al. 2000b).

Coral-based radiocarbon time series can be used not only to study oceanic processes, but also as a diagnostic tracer to test ocean circulation models (Guilderson et al. 2000a; Rodgers et al. 2000, among others). The bomb-radiocarbon acts as a natural perturbation experiment where the comparison of model results with observations of radiocarbon and other tracers is an effective way to identify problems or deficiencies in the model, and ultimately leads to improve modeling skill. The objective of this study is to examine the surface water radiocarbon variability in the southwest tropical Pacific as recorded in a hermatypic coral in the Solomon Sea in the context of understanding the lateral mixing that occurs in the western Pacific.

2. Site location

Guadalcanal (nominal location 9°S, 160°E) is located within the Solomon Island archipelago in the southwest tropical Pacific. The archipelago and Papua New Guinea to the north extend from the equator to ~10°S and provide the first physical barrier to westward flowing transpacific currents. Clear seasonal cycles are observed in the zonal and meridional local wind field with the mean wind being from the southeast quarter (DaSilva et al. 1994a). These southeast trade winds drive the off-equator branch (0–6°S) of the South Equatorial Current (SEC) that brings waters to the eastern side of the Solomon archipelago where it bends northward feeding both the central portion of the warm pool and southward into the South Equatorial Countercurrent (SECC; Fig. 1). At 165°E, eastward flowing waters of the SECC can be found between 6° and 11°S with maximum velocities between 8° and 9°S (Gouriou and Toole 1993). The position and intensity of this current varies seasonally in concert with the north–south migration of the South Pacific convergence zone (Gouriou and Toole 1993). Surface waters and currents inboard of the archipelago within the Solomon Sea (bounded to the west by Australia) are also dominated by the SEC influence. A second branch of the SEC feeds into the Coral and Solomon Seas through an extensive gap (approximately 11°–14°S) between the southernmost island of San Cristobal and the Banks Islands north of Vanuatu with some physical interference probably provided by the Santa Cruz Islands (see, e.g., Gouriou and Toole 1993; Reverdin et al. 1994). This current sweeps surface water of subtropical origin into the western Pacific.

Mean annual sea surface temperatures are ~29°C with only 1°–2°C seasonal variability (Levitus and Boyer 1994; Reynolds and Smith 1994). Mean annual salinity averages 34.6 psu with a seasonal range less than 1‰ (Levitus and Boyer 1994). The salinity and SST seasonal cycles are antiphased such that highest SSTs coincide with lowest salinities. This is a consequence of the correspondence of high SSTs and high precipitation being generally in phase (Fig. 2). Cumulative precipitation as recorded at Honiara [National Oceanic and Atmospheric Administration (NOAA) Global Historical Climatology Network (GHCN) station 9152000] is in excess of 2 m yr^{-1} with a clear wet–dry season differentiation. A climatological precipitation maximum of ~315 mm occurs in March (wet season: Dec–Apr) and a minima of ~83 mm in June (dry season: Jun–Sep). The average mixed layer depth in the Solomon Sea as defined by a 0.125 kg m^{-3} density contrast, is ~30 m with a seasonal range on the order of 10 m (Lukas and Lindstrom 1991; Monterey and Levitus 1997). On the other hand, using the 0.5°C criteria yields a mean on the order of 50 m with 20-m seasonal variability. The difference between the two is due to the impact of the high precipitation and lower salinity on the vertical density structure such that, although there is a relatively deep isothermal layer, the salinity difference results in some density stratification.

3. Analytical methods

A large (2.26 m) *Porites australiensis* coral head located off the southwestern side of Guadalcanal Island

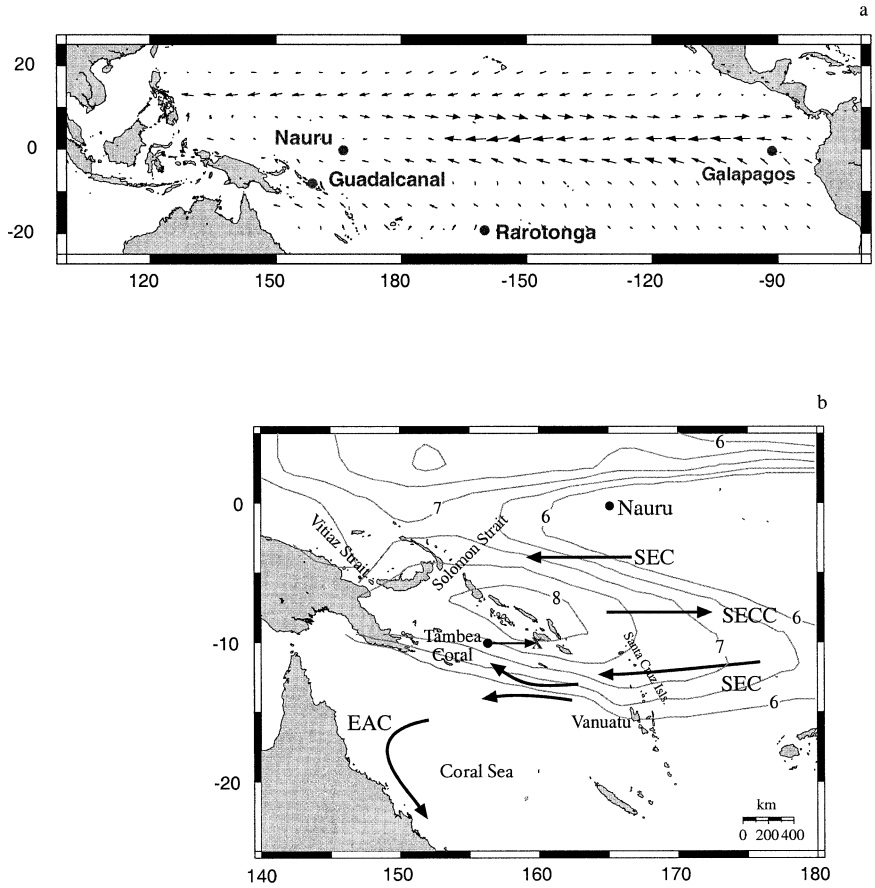

FIG. 1. (a) General surface circulation of the tropical Pacific based on current meter moorings and drifter data (after Reverdin et al. 1994) and coral locations discussed in the text. (b) Simplified surface circulation in the southwest tropical Pacific as described in the text, location of the Tambea (Guadalcanal) coral is designated with an X. Major surface currents influencing the region are the South Equatorial Current (SEC), South Equatorial Countercurrent (SECC), and the East Australian Current (EAC). Guadalcanal and the Solmon Sea are under the influence of the South Pacific convergence zone (SPCZ). Contour lines are daily precipitation (mm day^{-1}) derived from the Special Sensor Microwave Imager (SSM/I) passive microwave satellite measurements (Waliser and Gautier 1993) and demark the mean position of the SPCZ, the Indonesian low, and the intertropical convergence zone (north of the equator).

near Tambea Resort was drilled in July 1995. The cores (7.6 cm diameter) were cut into ~1 cm slabs, cleaned in distilled water, and air dried. No regions were infiltrated with boring filamentous algae or other organisms. After identifying the major vertical growth axis, the coral was sequentially sampled at 2-mm increments with a low-speed drill. Splits (~1 mg) were reacted in vacuo in a modified autocarbonate device at 90°C and the purified CO_2 analyzed on a gas source stable isotope ratio mass spectrometer. Analytical precision based on an in-house standard is better than $\pm 0.05‰$ (1σ) for both oxygen and carbon relative to the Vienna Pee Dee Belemnite (Coplen 1995).

Coral chronology has historically relied upon the presence of annual high- and low-density band couplets (e.g., Dodge and Vaisnys 1980 and references therein) or the seasonal variability in coral $\delta^{13}C$, which reflects surface irradiance (e.g., Fairbanks and Dodge 1979; Shen et al. 1992). Independent chronologies based on these two methods on the same coral specimen tend to agree within a few to six months (e.g., Shen et al. 1992; Guilderson and Schrag 1999). Such an age model is not adequate for high-resolution $\Delta^{14}C$ records where one of the ultimate goals is to compare the observed time series and those simulated in high-resolution ocean models (e.g., Rodgers et al. 2000). We created a preliminary age model based upon the seasonal structure within the $\delta^{13}C$ record but in order to obtain the best time scale, and because we are not interested in the coral $\delta^{18}O$ as an independent measure of precipitation or temperature, we have refined our age model by correcting the preliminary age model through coral $\delta^{18}O$ comparisons with instrumental records. To achieve this, we took our preliminary age model and filtered the $\delta^{18}O$ record to extract the annual component. The filtered record was then optimized by aligning the peaks and troughs re-

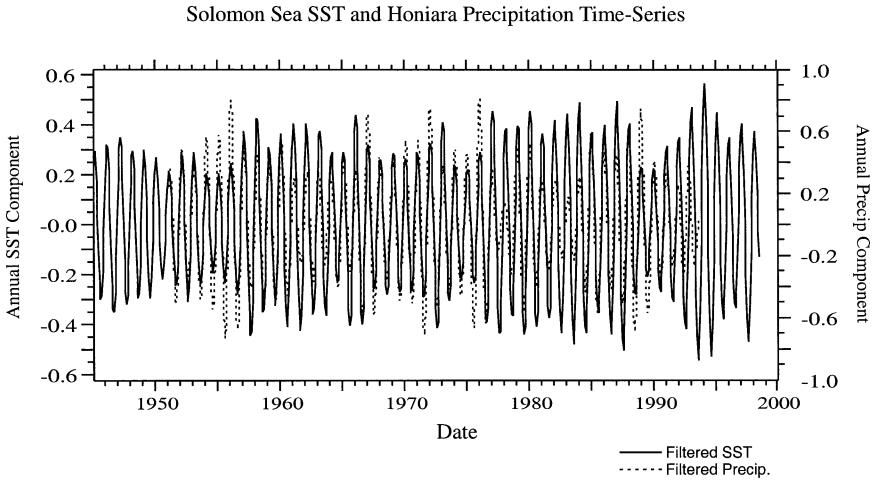

FIG. 2. Local instrumental data for Guadalcanal and the Solomon Sea. Monthly sea surface temperature (SST) data is a combination of the IGOSS satellite–ship of opportunity blended dataset (Reynolds and Smith 1984) and the Kaplan et al. (1998) reconstructed SST field for the grid box in the Solomon Sea containing Guadalcanal. Precipitation (dashed line) is from Honiara (NOAA GHCN station 9152000). Note that the seasonal cycle of each is in phase; highest SSTs correspond to higher times of higher rainfall.

flecting seasonal sea surface temperature and precipitation variations to instrumental records. We used a combination of the Integrated Global Ocean Station System (IGOSS; Reynolds and Smith 1994) blended satellite–ship of opportunity sea surface temperature record (1982–96) and that of the Kaplan et al. (1998) reconstructed SST (1850–1982) for the equivalent grid box containing the Tambea coral and the precipitation record from Honiara, which is nearly continuous from 1951–94. Between the tie-points reflecting seasonal maximum and minimum temperatures (and precipitation), the refined or tuned age model ($r = 0.84$ vs SST record) has an estimated error of ± 1.5 month (Fig. 3). Over the upper 1 m of the coral the refined age model varied by less than 5% from the original δ^{13}C-only age model.

The remaining sample splits (nominally 10 mg) from the upper 910 mm of the coral (corresponding interval 1942.65–1995.25) were placed in individual reaction chambers, evacuated, heated, and then acidified with orthophosphoric acid at 90°C. The evolved CO_2 was purified, trapped, and converted to graphite in the presence of a cobalt catalyst in individual reactors (Vogel et al. 1987). Graphite targets were measured at the Center for Accelerator Mass Spectrometry, Lawrence Livermore National Laboratory (Davis et al. 1990). Radiocarbon results are reported as age-corrected Δ^{14}C (‰)

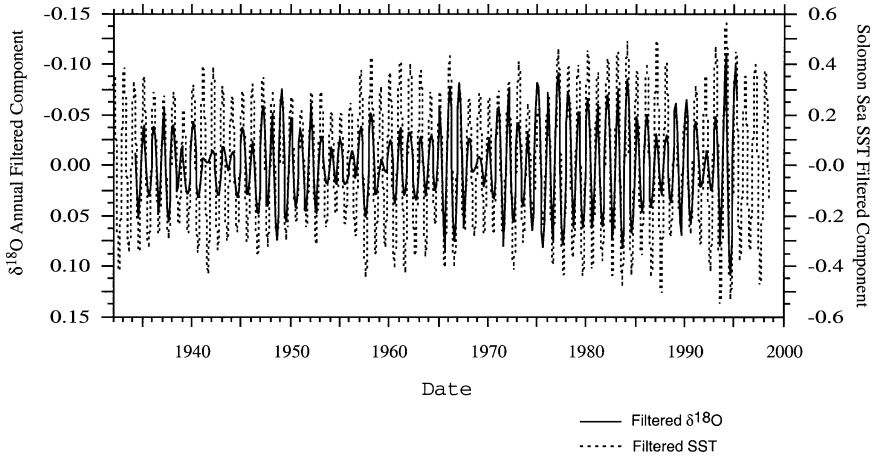

FIG. 3. Optimized coral δ^{18}O (solid line) and the instrumental sea surface temperature (dotted line) record ($r^2 = 0.71$ of the raw aligned data; $r^2 = 0.75$ of the filtered components).

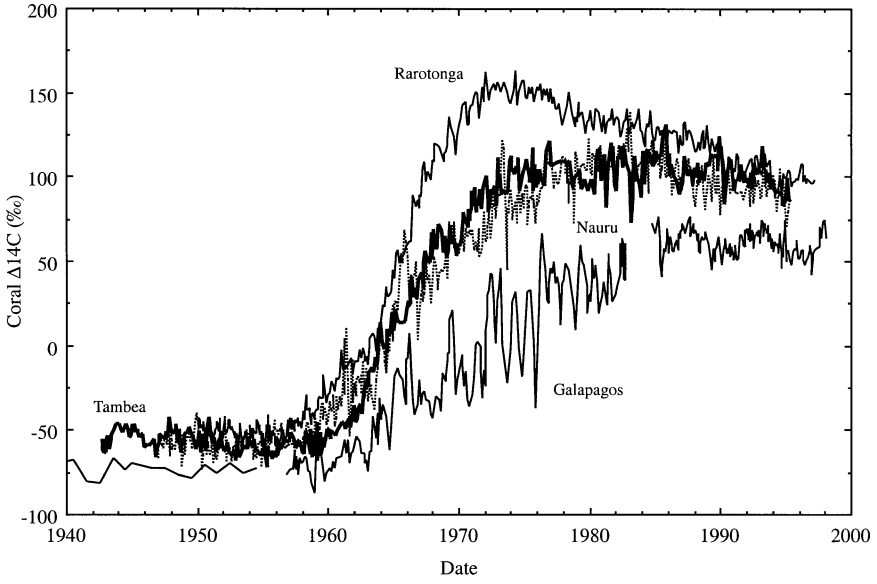

FIG. 4. Solomon Sea surface water $\Delta^{14}C$ (‰) as recorded in the Tambea coral. Individual (average 1.5-month sample resolution) values span a range from a low of −72‰ to a high of 132‰. Mean annual values range from −63‰ (1952) to 117‰ (1985). For comparison we have also plotted results from Nauru (0.5°S, 166°E; Guilderson et al. 1998); Rarotonga (20°S, 160°W; Guilderson et al. 2000b), and the Galapagos (Urvina Bay; Guilderson and Schrag 1998), and Wenman (T. P. Guilderson and D. P. Schrag 2000, unpublished manuscript). In a simple sense, the waters of the Solomon Sea reflect mixing of subtropical waters (Rarotonga) brought in from the southernmost branch of the SEC with water from the equatorward branch of the SEC whose origins lie in the eastern Pacific (Galapagos).

as defined by Stuiver and Polach (1977) and include the $\delta^{13}C$ correction obtained from the stable isotope results and a background subtraction determined on ^{14}C-free calcite. Analytical precision and accuracy of the radiocarbon measurements is ±4–5‰ (1σ) as monitored with an in-house homogenized coral standard and officially distributed secondary and tertiary radiocarbon standards.

4. Results

The surface water $\Delta^{14}C$ history as recorded in the Tambea coral is presented in Fig. 4 and over the length of the time series (1942.65–1995.25) has a dynamic range of ~200‰ from a low of −72‰ to a high of 132‰. Mean annual prebomb (1943–57) values are −56‰, similar to the values documented in a coral from Nauru Island ~9° to the north (0.5°S, 166°E; Guilderson et al. 1998). Over this 14-yr interval there is a linear decrease of nearly 1‰ yr^{-1} (−0.9‰ yr^{-1}, $r^2 = 0.62$). There is no seasonal cycle in $\Delta^{14}C$ during the prebomb period. Values are similar in 1957 and 1958 (−57‰) and by 1962 rose to −32‰. The largest single year increase occurred between 1962 and 1963 when values increased by 25‰ to −7‰. Except for 1969, where a slight (−3‰) decrease occurred, mean annual values continue to rise and by the early to mid-1970s reach 100‰. Like the record from Nauru, the postbomb peak occurs in the early 1980s: mean annual values peak in 1985 at 117%. The highest single value observed in the record of 132‰ also occurs in this year (1985.73). Between 1990 and 1993 mean annual values are nearly constant (~104‰) but in 1994 decrease to 90‰; 10–20‰ seasonal to interannual variability persists throughout the length of the record.

5. Discussion

Mean annual values decrease nearly 1‰ yr^{-1} over the 14 years immediately prior to the ''bomb era.'' Although this trend is consistent with the transfer of ^{14}C-free fossil fuel CO_2 into the ocean, the amplitude is much larger than previously documented or estimated in surface waters via simple one-dimensional modeling (e.g., Quay and Stuiver 1981; Druffel and Suess 1983). The length of the prebomb time series is insufficient to determine if the observed trend is biased by ocean dynamic variability. Low frequency or decadal variations in the shallow circulation of the Pacific influences the mixing of low ^{14}C subthermocline water with that of the mixed layer (Guilderson and Schrag 1998) and variability in the eastern Pacific could account for a portion of this signal.

The postbomb $\Delta^{14}C$ response of surface waters is directly related to the atmospheric forcing function of air–sea exchange (vis-a-vis equilibration kinetics) and ocean dynamics. The $\Delta^{14}C$ as measured in air samples from Wellington, New Zealand (Manning and Melhuish

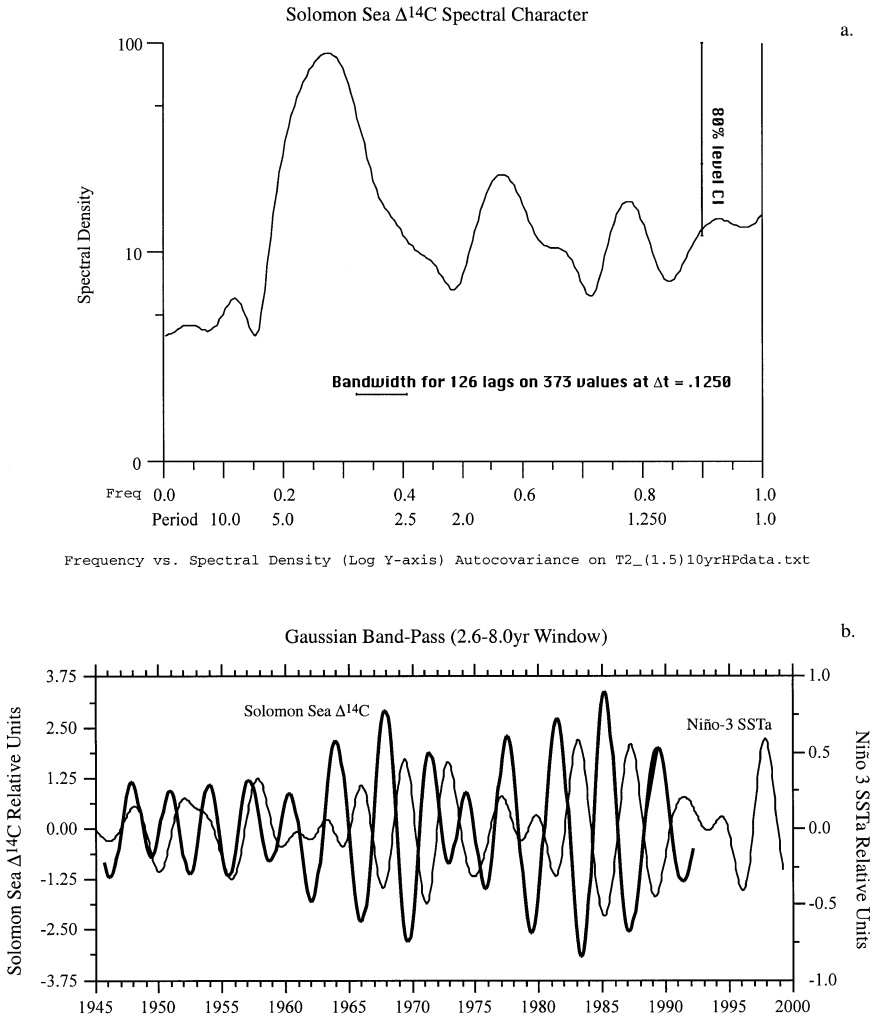

FIG. 5. Solomon Sea $\Delta^{14}C$ and the Niño-3 sea surface temperature records after Gaussian bandpass filtering at a central frequency of 0.25 ± 0.125 (2.6–8-yr window).

1994) shows an initial rise from ~−6‰ in 1955 to ~+33‰ in 1956 and 1957 and by 1959 values had risen to nearly +145‰. The atmospheric postbomb peak as recorded at Wellington occurred in 1965 (~+690). The Tambea $\Delta^{14}C$ record does not begin to rise significantly until late 1959 and reaches near-peak values (~104‰) in the early 1970s. Mean annual values remain relatively constant (±10‰) until the early 1990s with an annual maximum in 1985 of 117‰. The shape of the coral-based postbomb $\Delta^{14}C$ curve reflects the fact that waters of the Solomon Sea are predominantly of subtropical origin: subtropical (gyre) waters are relatively stable with high air–sea exchange rates and undergo comparatively less mixing with older subsurface waters, thus their $\Delta^{14}C$ content approaches equilibrium ''faster'' than other locations (e.g., Broecker and Peng 1982; Guilderson et al. 2000a). Superimposed upon the longer-term ''bomb-transient'' reflecting the uptake and redistribution of bomb-^{14}C are higher-frequency variations due to ocean dynamics.

The surface water radiocarbon history in the Tambea record reflects both near- and far-field circulation effects on seasonal to interannual time scales. On interannual time scales the record reflects the large-scale redistribution of surface waters during El Niño–Southern Oscillation and changes associated with the position of the South Pacific convergence zone. In the prebomb interval when surface $\Delta^{14}C$ gradients are smaller than in the postbomb, we may not expect to be able to resolve subtle variations in $\Delta^{14}C$ associated with the weak El Niño events of the 1950s. Future datasets from additional locations may allow us to place the prebomb $\Delta^{14}C$ variability in a better dynamic framework. We therefore focus our discussion on the postbomb interval when we are able to take full advantage of a large dynamic range in oceanic $\Delta^{14}C$. Comparison of a band-pass filtered version of this coral $\Delta^{14}C$ record with the canonical Niño-3 (5°S–5°N, 150°–90°W) sea surface temperature anomaly ENSO indicator (Fig. 5) implies little to no lag between the overlying wind field and the response of

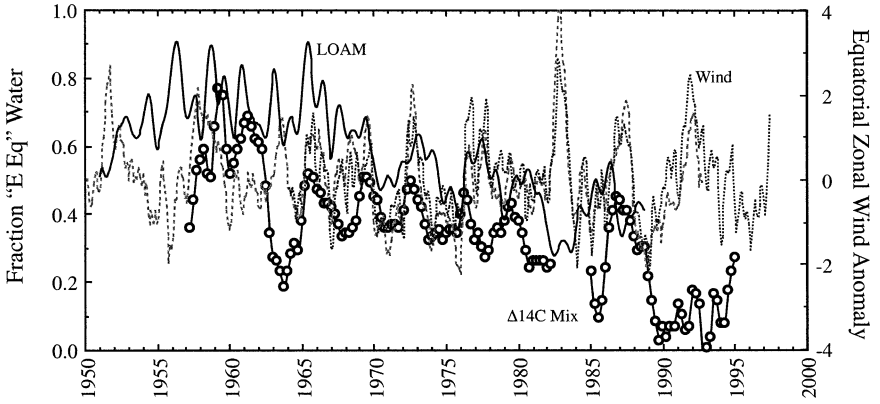

FIG. 6. Fraction of ''eastern Pacific'' water in the Solomon Sea derived from a simple two-end-member mixing model (open symbols, solid line), and a simple zonal wind *Z*-score anomaly near the date line using the detrended COADS data (dashed line: DaSilva et al. 1994a) and the FSU zonal wind stress (dotted line: Legler and O'Brien 1988). We have also plotted the equivalent Δ^{14}C-derived mixing model results for the Lamont ocean general circulation model (LOAM).

the transpacific surface ocean circulation. In general during the postbomb interval Δ^{14}C values are low when ENSO is in its warm phase (El Niño), and the converse is also true. There are some slight mismatches with the phasing, which we interpret to be the result of subtle differences in the physical manifestation of individual ENSO events; although in general each El Niño is similar, no event is exactly the same. Druffel and Griffin (1999) using ^{14}C data from Great Barrier Reef corals noted a similar correspondence of their record in conjunction with ENSO events. In the prebomb portion of the record and as a consequence of the weak Δ^{14}C gradient the sense of the relationship is less regular. Examination of ocean color images [from the Coastal Zone Color Scanner (CZCS)] in conjunction with historical hydrographic data (e.g., Lukas and Lindstrom 1991; Monterey and Levitus 1997) implies that in a climatological sense there is not a large amount of upwelling or vertical exchange in the Solomon Sea. High-quality SeaWifs data during the 1997–98 El Niño–La Niña cycle is consistent with the climatological picture (Murtugudde et al. 1999). We therefore interpret the Tambea ^{14}C time series to primarily reflect lateral advection and mixing of surface waters from the subtropics and the eastern tropical Pacific.

One of the underlying reasons to embark upon reconstructing detailed Δ^{14}C surface water time histories is to take advantage of Δ^{14}C as a quasi-conservative water parcel tracer. In a very simplified view, whereby the Solomon Sea Δ^{14}C is dominated by lateral advection processes, we can make a rough estimate of the relative proportion of tropical and extra-tropical surface water. We present the ^{14}C time series from Tambea with similar resolution results from Nauru in the center of the western tropical Pacific warm pool (0.5°S, 166°E; Guilderson et al. 1998), Rarotonga in the subtropics (20°S, 160°W; Guilderson et al. 2000b), and the Galapagos Islands (0°, 90°W; Druffel 1981; Guilderson and Schrag 1998; T. P. Guilderson and D. P. Schrag 2000, unpublished manuscript). Prebomb values, over the time frame common to all records (1950–57), at Rarotonga are −52‰ whereas values at Nauru are −58‰ and those from Tambea are −59‰ (Fig. 4). The SEC advects recently upwelled subthermocline (lower ^{14}C) water from the upwelling regions of the eastern and central tropical Pacific across the expanse of the Pacific, which results in the lower Δ^{14}C observed at Nauru (Guilderson et al. 1998) and in the Tambea (Guadalcanal) record. If we assume a simple two-end-member mixing model between southern subtropical (as reflected by the Rarotonga record) and eastern tropical water (i.e., Equatorial Undercurrent water in a base sense as reflected in the Galapagos record), the Solomon Sea contains 35%–40% eastern Pacific water. By using a surface record from the eastern Pacific low frequency variations in tropical thermocline dynamics, particularly the amount of entrainment of deeper less-ventilated water (see, e.g., Guilderson and Schrag 1998) are automatically accounted for. Although simplistic, such an estimate cannot be made utilizing temperature and salinity; neither of these properties is conservative in surface waters. Complications to this simplistic mixing approach come from entrainment/de-entrainment (laterally and vertically) of the end-member water masses from their respective ''source regions'' and variable mixing of more than two low Δ^{14}C end-member water masses. Thus our value is an upper estimate. We have applied this simple two-end-member mixing approach over the length of the respective coral-^{14}C records.

The corresponding ''deconvolved'' time series reinforces the interannual redistribution of Pacific surface waters due to ENSO (Fig. 6) with higher amounts of ''eastern Pacific'' water during the warm phase of ENSO. Quantitatively similar results as well as phasing with respect to the tropical wind field are obtained if one lags the Rarotonga and Galapagos time series prior

to performing the end-member mixing calculation to account for reasonable current velocities and transit times from the respective point sources (Reverdin et al. 1994; Johnson 2001). The rapid rise of atmospheric $\Delta^{14}C$ in the early 1960s precludes a strict interpretation of the mixing results during these few years when air–sea exchange dominates the surface water signal: due to higher air–sea gas exchange subtropical waters are more ''efficiently'' tagged with bomb radiocarbon and thus enhances the apparent importance of low ^{14}C water from the eastern tropical Pacific. It is our belief that the observation of apparently reduced SEC water during 1962–64 is an artifact of this process. Similarly efficient ''tagging'' of subtropical surface waters is observed in ocean circulation model studies using ^{14}C as a passive advective tracer (Rodgers et al. 2000; Guilderson et al. 2000a, among others).

It is perhaps too simple to resolve tropical Pacific dynamic variability in the context to a two-end-member mixing model and strictly relate all of the observed variability to ENSO. We are encouraged by the reasonably good visual correlation between our estimate of water mass mixing and ENSO but we also acknowledge that ENSO dynamics are not a panacea to explain all of the $\Delta^{14}C$ variability. Slight offsets between the Niño-3 SST and the fraction of eastern equatorial Pacific water in the Solomon Sea could be the result of ''inter-ENSO'' variability—whereby no El Niño event is exactly the same with respect to the absolute strength and intensity of the SEC and, of equal importance, could be variability as a result of a slight decoupling between the SPCZ and ENSO.

Repeat hydrographic sections at 137°E have documented a ~25% increase in the transport of the North Equatorial Current (NEC) and North Equatorial Countercurrent (NECC) between El Niño and non-El Niño years (Qiu and Joyce 1992). Unfortunately, such estimates do not exist for the equivalent repeat section to the east of the Solomons at 165°E (Gouriou and Toole 1993). During the warm phase of ENSO, the equatorial trade winds slacken (and/or reverse) and as a consequence, water that has normally been trapped in the warm pool of the western equatorial Pacific ''flows'' down the geopotential gradient to the east. Using satellite-derived surface topography and wind stress measurements Lagerloef et al. (1999) estimated near-surface currents during the 1997–98 El Niño event. They documented the complete reversal of the equatorial current with eastward flow on the order of 50 cm s^{-1}. Moreover, they observed a southward migration and intensification of the SEC in the westernmost portion of the Pacific in the spring of 1997 during the El Niño event. Our estimate of ''eastern tropical'' water is consistent with the southward migration and intensification of the SEC during the warm phase of ENSO. A similar conclusion was made by Druffel and Griffin (1995, 1999) where they observed decreased $\Delta^{14}C$ in surface waters along the Great Barrier Reef during El Niño events.

Comparison of the Tambea coral $\Delta^{14}C$ record with that from Nauru implies that in a very simple sense during the warm phase of ENSO there is not a corresponding redistribution of waters from the central portion of the western Pacific ''warm pool'' to the south: the Nauru coral $\Delta^{14}C$ is always higher than that of Tambea reflecting an increased influence of waters from the Northern Hemisphere (cf. Guilderson et al. 1998). This is an interesting observation because Nauru is within a half of a degree of the equator, and one would perhaps expect that its $\Delta^{14}C$ be lower due to subsequent advection of recently upwelled water along the equator. This observation reinforces the inference of asymmetry in the transport of waters from the eastern and central Pacific into the western Pacific: there is much transport south of the equator. The solution of the two-end-member mixing model indicates an overall decrease in the fraction of low-$\Delta^{14}C$ ''eastern equatorial Pacific'' water in the Solomon Sea. This observation may reflect an overall secular decrease in the intensity of upwelling in the eastern/central Pacific and the overall rate of tropical Pacific thermocline ventilation. We see a change in the upwelling season $\Delta^{14}C$ and sea surface temperature at the Galapagos when post-1976 there was less entrainment of deeper colder, low-^{14}C water (Guilderson and Schrag 1998). However, our estimate of the fraction of eastern equatorial Pacific water accounts for this change since it is based on the surface expression of this physical process. If the interpretation of our observations and those of Lagerloef et al. (1999) are indeed accurate, the increase in the intensity and frequency of El Niño events over the last 20 years would increase the influence of the equatorward branch of the SEC on the Solomon Sea, and the $\Delta^{14}C$ values should be more similar to those of the eastern Pacific. This is not what we observe, where we calculate a decrease in the influence of low ^{14}C water from the eastern equatorial Pacific over the latter stages of the twentieth century.

The surface $\Delta^{14}C$ variations that we have documented reflect not only the interannual variability but also the gross overturning of the shallow tropical Pacific circulation and tropical Pacific thermocline ventilation (Wyrtki and Kilonsky 1984; Toggweiler et al. 1991). As documented by Toggweiler et al. (1991) and Guilderson and Schrag (1998), the water masses involved in the ventilation of the tropical Pacific thermocline extend to at least 10°C and large volumes of water are involved (Wyrtki and Kilonsky 1984). The surface expression of the variability in temperature is masked by constant air–sea exchange making it problematic to reconstruct the circulation from records of sea surface temperature. Surface variations in $\Delta^{14}C$ are not reset due to the isotopic equilibriation time between the ocean and atmosphere (~10 yr). The records that we present here imply that there has been an overall reduction in the overall turnover of the tropical Pacific thermocline. This interpretation is supported by the recent work of McPhaden and

Zhang (2002) who reached a similar conclusion using historical hydrographic profiles.

Detailed data–model comparisons using coupled ocean models with sufficient resolution that accurately portray equatorial Pacific dynamics will be necessary to further confirm this observation. Current ocean models have systematic errors that do not allow for a precise comparison using ^{14}C. In the upwelling region of the eastern equatorial Pacific most ocean models upwell water from too deep a depth, yielding not only a cold bias to sea surface temperatures but also an inaccurate $\Delta^{14}C$ time history (e.g., Rodgers et al. 1999; Guilderson et al. 2000a). Insufficient vertical mixing in the subtropics, presumably poor parameterization of winter storm events, results in a ''pile-up'' of bomb ^{14}C in the surface mixed layer—peak values occur too soon and values are too high (e.g., Rodgers et al. 1999; Guilderson et al. 2000a). A similar end-member mixing analyses of results for the grid boxes equivalent to the coral locations generated in the Lamont high-resolution ocean general circulation forced with observed winds and a fixed Indonesian Throughflow transport (Rodgers et al. 1999) does indeed exhibit a secular decrease in the proportion of eastern equatorial Pacific water in the Solomon Sea. The fact that the model recreates the observed secular trend could perhaps be a fortuitous result but we think that it is more likely the result of forcing the high-resolution model with the observed wind field. The modeled secular trend reinforces the tight coupling between the atmosphere and the wind-driven portion of the ocean. The model does a reasonably good job of the lateral redistribution of surface waters and hence the overall simulated tracer field. However, the interannual variability is counter to that which we observe. This is in large part, due to the problems and difficulty of accurately recreating the dynamics and the $\Delta^{14}C$ of the eastern equatorial Pacific and winter mixing in subtropical gyres (cf. Fig. 13 in Rodgers et al. 1999).

6. Conclusions

We have reconstructed the surface water radiocarbon history of the Solomon Sea as recorded in a hermatypic coral recovered off Guadalcanal. Over the interval 1943–57 the mean annual value is −56‰ with a linear decrease of nearly 1‰ yr^{-1}. Although consistent with the Suess effect, the record is too short to ascertain how much of the trend is influenced by interannual to decadal-scale ocean dynamic variability. The postbomb maximum occurs in 1985 with a value of 117‰. Interannual variability in the record reflects the distribution of water masses associated with ENSO.

A simple mixing model between southern subtropical and eastern tropical water is constructed that indicates during El Niño events there is more water of eastern Pacific origin in the Solomon Sea. This is most easily accomplished by a southward migration of the equatorial branch of the SEC during the warm phase of ENSO, an interpretation corroborated by satellite observations during the 1997–98 ENSO. There is a secular trend in the mixing model results, which imply that the intensity of the shallow overturning cell of the tropical Pacific has decreased over the last ~20 years.

Acknowledgments. Collection of the Tambea coral would not have been possible without the assistance of M. D. Moore. We would like to thank E. Stokely for allowing TG free reign in CAMS' graphite preparation laboratory and B. Frantz, J. Westbrook, and P. Zermeno for pressing the majority of the graphite targets. Stable isotope analyses were performed at the Laboratory for Geochemical Oceanography, Harvard University by E. Goddard. The ''Arand'' spectral package is maintained and distributed by Phil Howell, Brown University. This manuscript benefited from discussions with G. Johnson, R. Murtugudde, K. Rodgers, and thoughtful and constructive comments by M. Mann, R. Toggweiler, and two unknown reviewers. This work was supported by a UCOP/CAMS minigrant, and grants to T. Guilderson and M. Kashgarian (LLNL 98-ERI-002) and to D. Schrag (OCE-9796253) and M. Cane (OCE-9633375) from NSF's program in Physical and Chemical Oceanography. Radiocarbon analyses were performed under the auspices of the U.S. Department of Energy by the University of California Lawrence Livermore National Laboratory (Contract W-7405-Eng-48). Data will be digitally archived at NOAA's World Data Center-A (Boulder, Colorado).

REFERENCES

Broecker, W. S., and T.-H. Peng, 1982: *Tracers in the Sea.* ELDIGIO Press, 690 pp.

Clarke, A. J., and A. Lebedev, 1996: Long-term changes in the equatorial Pacific trade winds. *J. Climate,* **9,** 1020–1029.

Coplen, T. B., 1995: Discontinuance of SMOW and PDB. *Nature,* **375,** 285.

DaSilva, A., C. C. Young, and S. Levitus, 1994a: *Algorithms and Procedures.* Vol. 1, *Atlas of Surface Marine Data 1994,* NOAA Atlas NESDIS 6, 83 pp.

Davis, J. C., and Coauthors, 1990: LLNL/UC AMS facility and research program. *Nucl. Instrum. Methods Phys. Res.,* **52B,** 269–272.

Dodge, R. E., and J. R. Vaisnys, 1980: Skeletal growth chronologies of recent and fossil corals. *Skeletal Growth of Aquatic Organisms,* D. C. Rhoads and R. A. Lutz, Eds., Topics in Geobiology, Vol. 1, Plenum, 493–517.

Druffel, E. M., 1981: Radiocarbon in annual coral rings from the eastern tropical Pacific Ocean. *Geophys. Res. Lett.,* **8,** 59–62.

——, and H. E. Suess, 1983: On the radiocarbon record in banded corals: Exchange parameters and net transport of $^{14}CO_2$ between atmosphere and surface ocean. *J. Geophys. Res.,* **88,** 1271–1280.

——, and S. Griffin, 1995: Regional variability of surface ocean radiocarbon from southern Great Barrier Reef corals. *Radiocarbon,* **37,** 517–524.

——, and ——, 1999: Variability of surface ocean radiocarbon and stable isotopes in the southwestern Pacific. *J. Geophys. Res.,* **104,** 23 607–23 613.

Fairbanks, R. G., and D. Dodge, 1979: Annual periodicity of the $^{18}O/^{16}O$ and $^{13}C/^{12}C$ ratios in the coral Montastrea annularis. *Geochim. Cosmochim. Acta,* **43,** 1009–1020.

Goriou, Y., and J. Toole, 1993: Mean circulation of the upper layers of the western equatorial Pacific Ocean. *J. Geophys. Res.,* **98,** 22 495–22 520.

Guilderson, T. P., and D. P. Schrag, 1998: Abrupt shift in subsurface temperatures in the eastern tropical Pacific associated with recent changes in El Niño. *Science,* **281,** 240–243.

——, and ——, 1999: Reliability of coral records from the western Pacific warm pool: A comparison using age-optimized records. *Paleoceanography,* **14,** 457–464.

——, ——, M. Kashgarian, and J. Southon, 1998: Radiocarbon variability in the western equatorial Pacific inferred from a high-resolution coral record from Nauru Island. *J. Geophys. Res.,* **103,** 24 641–24 650.

——, D. P. Schrag, E. Goddard, M. Kashgarian, G. M. Wellington, and B. K. Linsley, 2000b: Southwest subtropical Pacific surface radiocarbon in a high-resolution coral record. *Radiocarbon,* **42,** 249–256.

——, K. Caldeira, and P. B. Duffy, 2000a: Radiocarbon as a diagnostic tracer in ocean and carbon cycle modeling. *Global Biogeochem. Cycles,* **14,** 887–902.

Johnson, G. C., 2001: The Pacific Ocean subtropical cell surface limb. *Geophys. Res. Lett.,* **28,** 1771–1774.

Kaplan, A. M., M. Cane, Y. Kushnir, A. C. Clement, M. B. Blumenthal, and B. Rajagopalan, 1998: Analyses of global sea surface temperature 1856–1991. *J. Geophys. Res.,* **103,** 18 567–18 589.

Key, R. M., P. D. Quay, G. A. Jones, A. P. McNichol, K. F. Von Reden, and R. J. Schneider, 1996: WOCE AMS radiocarbon I: Pacific Ocean results (P6, P16, and P17). *Radiocarbon,* **38,** 425–518.

Lagerloef, G. S. E., G. T. Mitchum, R. B. Lukas, and P. P. Niiler, 1999: Tropical Pacific near-surface currents estimated from altimeter, wind, and drifter data. *J. Geophys. Res.,* **104,** 23 313–23 326.

Legler, D. M., and J. J. O'Brien, 1988: Tropical Pacific wind stress analysis for TOGA. *IOC Time Series of Ocean Measurements.* IOC Tech. Series 33, UNESCO, Vol. 4, 11–17.

Levitus, S., and T. Boyer, 1994: *Temperature.* Vol. 4, *World Ocean Atlas 1994,* NOAA Atlas NESDIS 4, 117 pp.

Lukas, R., and E. Lindstrom, 1991: The mixed layer of the western equatorial Pacific. *J. Geophys. Res.,* **96,** 3343–3357.

Luther, D. S., and D. E. Harrison, 1984: Observing long-period fluctuations of surface winds in the tropical Pacific: Initial results from island data. *Mon. Wea. Rev.,* **112,** 285–302.

Manning, M. R., and W. H. Melhuish, 1994: Atmospheric $\Delta^{14}C$ record from Wellington. *Trends '93: A Compendium of Data on Global Change,* T. A. Boden et al., Eds., Carbon Dioxide Information Analysis Center, Oak Ridge National Laboratory, Publ. ORNL/CDIA C65, 193–202.

McPhaden, M. J., and D. Zhang, 2002: Slowdown of the meridional overturning circulation in the upper Pacific Ocean. *Nature,* **415,** 603–608.

Monterey, G. I., and S. Levitus, 1997: *Seasonal Variability of Mixed Layer Depth for the World Ocean.* NOAA Atlas NESDIS 14, U.S. Gov. Printing Office, 5 pp.

Murtugudde, R., S. Signorini, J. Christian, A. Busalacchi, and C. McClain, 1999: Ocean color variability of the tropical Indo-Pacific basin observed by SeaWiFS during 1997–98. *J. Geophys. Res.,* **104,** 18 351–18 366.

Östlund, H. G., H. Craig, W. S. Broecker, and D. Spencer, 1987: *GEOSECS Atlantic, Pacific, and Indian Ocean Expeditions.* Vol. 7, National Science Foundation 200 pp.

Peixoto, J. P., and A. H. Oort, 1992: *Physics of Climate.* American Institute of Physics, 520 pp.

Quay, P. D., and M. Stuiver, 1981: Atmospheric C-14 changes resulting from fossil fuel CO_2 release and cosmic-ray flux variability. *Earth Planet. Sci. Lett.,* **53,** 349–362.

Qiu, B., and T. M. Joyce, 1992: Interannual variability in the mid- and low-latitude western North Pacific. *J. Phys. Oceanogr.,* **22,** 1062–1079.

Reverdin, G., C. Frankignoul, E. Kestenare, and M. J. McPhaden, 1994: Seasonal variability in the surface currents of the equatorial Pacific. *J. Geophys. Res.,* **99,** 20 323–20 344.

Reynolds, R. W., and T. M. Smith, 1994: Improved global sea surface temperature analyses. *J. Climate,* **7,** 929–948.

Rodgers, K. B., D. P. Schrag, M. A. Cane, and N. H. Naik, 2000: The bomb C-14 transient in the Pacific Ocean. *J. Geophys. Res.,* **105,** 8489–8512.

Shen, G. T., L. J. Linn, T. M. Campbell, J. E. Cole, and R. G. Fairbanks, 1992: A chemical indicator of trade wind reversal in corals from the western tropical Pacific. *J. Geophys. Res.,* **97,** 12 689–12 697.

Stuiver, M., and H. A. Polach, 1977: Discussion and reporting of ^{14}C data. *Radiocarbon,* **19,** 355–363.

Toggweiler, J. R., K. Dixon, and W. S. Broecker, 1991: The Peru upwelling and the ventilation of the South Pacific thermocline. *J. Geophys. Res.,* **96,** 20 467–20 497.

Vogel, J. S., J. R. Southon, and D. E. Nelson, 1987: Catalyst and binder effects in the use of filamentous graphite for AMS. *Nucl. Instrum. Methods Phys. Res.,* **29B,** 50–56.

Waliser, D. E., and C. Gautier, 1993: A satellite–derived climatology of the ITCZ. *J. Climate,* **6,** 2162–2174.

Wyrtki, K., and B. Kilonsky, 1984: Mean water and current structure during the Hawaii to Tahiti shuttle experiments. *J. Phys. Oceanogr.,* **14,** 242–254.